Roundabout model with on-ramp queues: Exact results and scaling approximations

P. J. Storm,[*] S. Bhulai,[†] and W. Kager[‡]
Vrije Universiteit, 1081 HV Amsterdam, The Netherlands

M. Mandjes[§]
University of Amsterdam, 1012 WX Amsterdam, The Netherlands

This paper introduces a general model of a single-lane roundabout, represented as a circular lattice that consists of L cells, with Markovian traffic dynamics. Vehicles enter the roundabout via on-ramp queues that have stochastic arrival processes, remain on the roundabout a random number of cells, and depart via off-ramps. Importantly, the model does not oversimplify the dynamics of traffic on roundabouts, while various performance-related quantities (such as delay and queue length) allow an analytical characterization. In particular, we present an explicit expression for the marginal stationary distribution of each cell on the lattice. Moreover, we derive results that give insight on the dependencies between parts of the roundabout, and on the queue distribution. Finally, we find scaling limits that allow, for every partition of the roundabout in segments, to approximate (i) the joint distribution of the occupation of these segments by a multivariate Gaussian distribution, and (ii) the joint distribution of their total queue lengths by a collection of independent Poisson random variables. To verify the scaling limit statements, we develop a way to empirically assess convergence in distribution of random variables.

I. INTRODUCTION

Over the past decades, a broad class of models has been proposed to better understand and control traffic streams in road traffic networks. This has led to mathematical models that help shed light on the properties of the underlying traffic dynamics. In particular, these models allow for studying the influence of the model's parameters, which in turn allows for developing effective design and control rules. For reviews on traffic flow theory, see, e.g., [1,2], and for cellular automata models used in this area, see [3]. In the literature on traffic flows, most mathematical analyses are done for road segments and several forms of intersection traffic control, i.e., signalized intersections and unsignalized intersections with or without priorities.

Roundabouts are a type of intersection that is notoriously hard to analyze mathematically. Fouladvand *et al.* [4] studied the delay experienced by traffic in roundabouts in relation to their geometry by simulating a stochastic cellular automata model. Wang and Ruskin [5], Wang and Liu [6], and Belz *et al.* [7] studied the capacity of cellular automata roundabout models incorporating the traffic behavior of individual cars in a more sophisticated manner. In these models, the analysis focuses on the relationship between the circulating flow and the capacity of an entry road at the roundabout. The conclusions are primarily based on simulation results, and

hence do not provide explicit insight into, e.g., the way the system parameters affect the capacity or delay.

In addition, there are a number of analytical papers studying the relationship between circulating flow and capacity at an entry road. For example, Flannery *et al.* [8,9] have obtained an analytical approximation of this relationship based on earlier work for unsignalized intersections by Tanner [10] and Heidemann and Wegmann [11]. For these results, vehicles are assumed to be separated by i.i.d. distributed gaps, so that on-ramps can be modeled as $M/G/1$ queues. However, this approach studies queues in isolation, and ignores the interaction of on-ramps being connected to a circular ring. Finally, in a recent paper, Foulaadvand *et al.* [12] derived exact stationary densities for the occupation of a roundabout, with traffic motion modeled by the totally asymmetric exclusion process, but, importantly, without queueing at the entry roads.

Summarizing, many studies are based on simulation models or regression analyses (Ref. [13], Chap. 21), thus not providing direct insight into the impact of the model parameters. On the other hand, analytical studies tend to study parts of the roundabout in isolation, ignoring characteristic geometric properties of roundabouts. The primary contribution of this paper is a single-lane roundabout model that (i) is still analytically tractable, and (ii) still contains the detailed geometric properties of the underlying system. More specifically, we set up a model in which we succeed in deriving (a) an exact marginal stationary distribution for the occupation of the roundabout; (b) results on the dependencies between parts of the roundabout, and on the queue distribution; and (c) scaling limits for the occupation of the roundabout and the states of the queues. Our results lead to a better understanding of traffic dynamics in roundabouts, and, in particular, of the effects of

[*]p.j.storm@vu.nl
[†]s.bhulai@vu.nl
[‡]w.kager@vu.nl
[§]m.r.h.mandjes@uva.nl

model parameters on performance. As a consequence, our findings have evident application potential when setting up procedures for design and control. A second main contribution relates to the verification of properties (b) and (c) above, for which we rely on simulation: we develop a procedure to statistically assess convergence in distribution.

The outline of the paper is as follows. In Sec. II, we introduce the model. In Sec. III, we identify the exact marginal stationary distribution for the occupation of the roundabout, and we discuss why it is difficult to derive further analytic results. Our methods, which are used in later sections, are explained in Sec. IV. Section V contains results on intrinsic model properties, whereas in Secs. VI and VII we study scaling results.

II. MODEL DESCRIPTION

The model we consider is a road traffic model for a roundabout with (on-ramp) queues at the points of entrance into the roundabout. The exit point of a car from the roundabout is random and depends on its point of entry. The roundabout is modeled as a stretch of road consisting of L cells numbered $1, \dots, L$, which we assume to be arranged in a circle, so that cell 1 is adjacent to cell L. Making use of this circularity, we will also use the index $L + i$ to refer to cell i, for $1 \leqslant i \leqslant L$, to simplify notation. Each cell can contain at most one car, and to keep track of the cars in the roundabout, we attach the state space $\{0, 1, \dots, L\}$ to each cell: state 0 indicates that a cell is vacant, and a state $j \in \{1, \dots, L\}$ indicates that the cell is occupied by a car that entered the roundabout at cell j. For ease of reference, we will also say that a cell is occupied by a car of *type* j if the state of the cell is j.

The main characteristics of the evolution of our stochastic system are the following. To model how cars get into the roundabout, we assume that there is an on-ramp queue in front of each cell i. At every time step, a new car arrives at the queue of cell i with probability $p_i \in [0, 1]$. From this queue, in every time step, a single car can move into the roundabout, but only when cell i is empty. If cell i is occupied by a car of type j at a specific moment in time, then with probability $q_{ij} \in [0, 1]$ the car will leave the roundabout in the next time step (and otherwise it moves to the next cell). The fact that the probability q_{ij} depends on j reflects that, in general, the position where a car leaves the roundabout can depend on where it entered. Note that by setting $p_i = 0$ or $q_{ij} = 0$ we can remove on-ramps and off-ramps from the system, and thus flexibly model their position.

Now that we have sketched the main principles behind our model, we proceed by providing a more precise account of the dynamics. A key feature of the model is that the update rules (given in detail below) are *local*, meaning that at each time step, we can consider what happens at each of the cells of the model independently, and then update all the local states in parallel (in accordance with the cellular automata paradigm). Thus it suffices to describe what happens at a single cell and the corresponding queue. We distinguish between the following cases:

Case 1: Cell i and queue i are both empty. In this case, if no new car arrives at cell i (which happens with probability $1 - p_i$), then cell $i + 1$ and queue i will both be empty at the

next time step. Otherwise, the newly arrived car immediately enters the roundabout and moves on to cell $i + 1$, meaning that cell $i + 1$ will be in state i at the next time step, and queue i will still be empty.

Case 2: Cell i is empty and queue i is not empty. In this case, the first car waiting in queue i enters the roundabout and moves on to cell $i + 1$. Thus, cell $i + 1$ will be in state i at the next time step, and the length of queue i will either decrease by 1 (if no new car arrives at cell i), or otherwise stay the same.

Case 3: Cell i is occupied by a car of type j. In this case, queue i is blocked, and hence its length will stay the same if no new car arrives at cell i, or otherwise grow by 1. Meanwhile, the car of type j can decide to leave the roundabout (which it does with probability q_{ij}), in which case cell $i + 1$ will be empty at the next time step, or the car decides to drive on, in which case cell $i + 1$ will be in state j at the next time step.

III. PRELIMINARIES

The model under consideration is a discrete-time Markov chain, the state of which is a vector describing the state of each cell and the length of each queue. We will denote the Markov chain by $X = \{X_t : t \in \mathbb{Z}_+\}$. It is not difficult to see that X is irreducible and aperiodic, since with positive probability, by choosing the right events, we can empty the system in a finite number of steps, keep it in the empty state for an arbitrary number of steps, and then send it to any state we like in a finite number of steps.

We say that the model is *stable* if the Markov chain X is positive recurrent, and hence has a unique stationary distribution. As our first result, we will now show that, under the assumption of stability, the marginal stationary probability π_{ij} that a given cell i is in state j is given by

$$
\pi_{ij} = \begin{cases} \dfrac{p_j \prod_{\ell=j+1}^{i+L-1} \bar{q}_{\ell j}}{1 - \prod_{\ell=1}^{L} \bar{q}_{\ell j}} & \text{if } 1 \leqslant i \leqslant j \leqslant L, \\[4mm] \dfrac{p_j \prod_{\ell=j+1}^{i-1} \bar{q}_{\ell j}}{1 - \prod_{\ell=1}^{L} \bar{q}_{\ell j}} & \text{if } 1 \leqslant j < i \leqslant L, \end{cases} \tag{1}
$$

where $\bar{q}_{\ell j} := 1 - q_{\ell j}$, and

$$
\pi_{i0} = 1 - \sum_{j=1}^{L} \pi_{ij}, \quad 1 \leqslant i \leqslant L. \tag{2}
$$

Proposition III.1 (Marginal stationary distribution). If the model is stable, then the marginal stationary probability that cell i is in state j is given by (1) and (2).

Proof. Assume that the model is stable, and first consider the case in which i and j satisfy $1 \leqslant j < i \leqslant L$. Then the probability that a car that enters the roundabout at cell j will leave at cell i (potentially after first completing $n \geqslant 0$ full circles in the roundabout) is given by

$$
q_{ij} \prod_{\ell=j+1}^{i-1} \bar{q}_{\ell j} \sum_{n=0}^{\infty} \left(\prod_{\ell=1}^{L} \bar{q}_{\ell j} \right)^n = \frac{q_{ij} \prod_{\ell=j+1}^{i-1} \bar{q}_{\ell j}}{1 - \prod_{\ell=1}^{L} \bar{q}_{\ell j}}.
$$

We conclude that this expression multiplied by p_j is the rate at which cars arrive that are of type j, and that intend to leave the roundabout at cell i. But if the model is stable, then the rate at which such cars leave the system must be equal to $\pi_{ij}q_{ij}$, where π_{ij} denotes the marginal stationary probability that cell i contains a car of type j. This proves (1) when $j < i$. The proof in the case $1 \leqslant i \leqslant j \leqslant L$ is similar.

Even though we now have an exact expression for the marginal stationary distribution of the cells, the full joint stationary distribution of the Markov chain X cannot be found. In particular, the stationary distribution will not be the product distribution of the marginals of the cells and queues. Indeed, consider the event in which queue i and cell $i + 1$ are both empty for some $i \in \{1, \dots, L\}$. Then, one time unit earlier queue i must have been empty, because otherwise, either queue i would now still be nonempty, or a car from queue i would now be in cell $i + 1$. This shows that there is a dependency in the model between adjacent cells and queues, ruling out a product-form stationary distribution.

To conclude this section, we discuss the model's stability condition. We have shown above that when the model is stable, π_{i0} is the stationary probability at which cell i is empty. Since cars arrive at cell i with probability p_i, and can only enter the roundabout when the cell is empty, it is conceivable that the model cannot be stable if $p_i \geqslant \pi_{i0}$ for some cell i. Conversely, one suspects that if $p_i < \pi_{i0}$ for all cells i, then the cells will be vacant often enough to prevent the queue lengths from growing arbitrarily large, and hence the model will be stable. We have tested this conjecture using extensive simulation experiments in which we replace p_i by αp_i and increase α (starting from $\alpha = 0$). The experiments confirm that a system becomes unstable when α exceeds the smallest value for which $\alpha p_i \geqslant \pi_{i0}(\alpha)$ for some $i \in \{1, \dots, L\}$. Throughout Secs. IV–VII, we therefore restrict ourselves to cases in which $p_i < \pi_{i0}$ for all $i \in \{1, \dots, L\}$.

IV. METHODS

Since we do not have a closed-form expression for the joint stationary distribution, we resort to finding approximations for the stationary distributions of cells and queues. More specifically, in Sec. II we introduced the p_i and q_{ij}, which can be seen as discrete profiles of arrival and departure probabilities (as a function of the position i between 1 and L). In Sec. IV A, we introduce their continuous counterparts, so that for finite L, the p_i and q_{ij} are obtained as discretizations of these continuum profiles. The continuous setting allows explicit analysis, with which we can approximate our discrete model.

Later in the paper (in Secs. VI and VII) we state claims on, respectively, the number of empty cells and the total queue length for each section of the roundabout in the regime $L \to \infty$. To verify these claims from simulation experiments, we develop a methodology, which is described in Sec. IV B.

A. Continuum profiles and parameters

We proceed by introducing the continuum profiles of arrivals and departures. We start with the arrivals. Let $\varrho : (0, 1] \to \mathbb{R}^+$ be an integrable function that satisfies $\int_0^1 \varrho(x)dx = 1$. For given $L \in \mathbb{Z}^+$, $\theta > 0$, and $i \in \{1, \dots, L\}$,

we set

$$p_i \equiv p_i(L) = \theta \int_{i/L}^{(i+1)/L} \varrho(x)dx.$$

This construction can be interpreted as follows. When taking the limit $L \to \infty$, the circular stretch of road is mapped onto the unit interval $(0,1]$. The parameter $\theta > 0$ represents the total rate at which cars arrive at the roundabout, and for a given interval $(u, v] \subset (0, 1]$, $\int_u^v \varrho(x)dx$ represents the rate at which cars arrive in that interval. Informally, for L large, p_i is roughly proportional to L^{-1}. Note that in this setup, the arrival rate over every segment of the roundabout is invariant in L.

To describe the continuum profile for the departures, we introduce a family $[F_x(\cdot)]_{x \in (0,1]}$ of cumulative distribution functions on $[0,1]$ [which are nondecreasing with $F_x(0) = 0$], and we denote by $F_x^c(\cdot) \equiv 1 - F_x(\cdot)$ their complementary distribution functions. The idea is that in the limit $L \to \infty$, $F_x^c(u)$ represents the probability that a car that enters the roundabout at point x travels at least a distance u along the roundabout before leaving. For each finite $L \in \mathbb{Z}_+$ and $i, j \in \{1, \dots, L\}$, we now set

$$q_{ij} \equiv q_{ij}(L) = \begin{cases} 1 - \dfrac{F_{j/L}^c[(i-j+1)/L]}{F_{j/L}^c[(i-j)/L]}, & i \geqslant j, \\[4mm] 1 - \dfrac{F_{j/L}^c[(L+i-j+1)/L]}{F_{j/L}^c[(L+i-j)/L]}, & i < j. \end{cases}$$

Since we interpret $F_{j/L}$ as the distribution function of the driving distance for cars arriving at j/L, $1 - q_{ij}(L)$ for $i \geqslant j$ can be seen as the conditional probability that such a car drives at least a distance $(i - j + 1)/L$ in the roundabout, given that the car has driven a distance $(i - j)/L$, and similarly for $i < j$. Hence the above definition of q_{ij} guarantees that the distribution of driving distance of cars remains invariant in L. We further assume that F_x^c is piecewise continuous as a function of x, meaning that cars that arrive at roughly the same place in the roundabout also have roughly the same distribution of driving distance. This condition is natural, and it guarantees the existence of $\lim_{L \to \infty} \pi_{\lceil uL \rceil, 0}$.

To summarize: for given ϱ and a family of F_x, we obtain a sequence of models in L, which can be viewed as discrete representations of the same roundabout. In the remainder of the paper, we consider two specific cases of continuum profiles and the discrete models they produce for different values of L, in order to support the claims we make in Secs. V, VI, and VII.

Most of the arguments by which we arrive at our claims are based on the symmetric case in which $p_i = p \in (0, 1)$ and $q_{ij} = q \in (0, 1)$ for each $i, j \in \{1, \dots, L\}$. We therefore choose a parameter setting in this symmetric case such that $\pi_{i0} > p_i$. More specifically, we choose $\varrho(x) = 1$ with $\theta = 1$, and $F_x^c(u) = \exp(-2u)$ for each $x \in (0, 1]$, so that for finite L we have $p(L) = 1/L$ and $q(L) = 1 - \exp(-2/L)$. We refer to this choice as the *homogeneous setting* or the *homogeneous case*.

To illustrate that our claims are also supported in a realistic nonhomogeneous case, we use an example from [13] (Chap. 21), namely Example Problem 1. This example describes a roundabout with four on-/off-ramps, and it gives for each on-ramp (i) the number of arrivals per hour, and (ii) the fraction of arriving cars that depart via each of the four
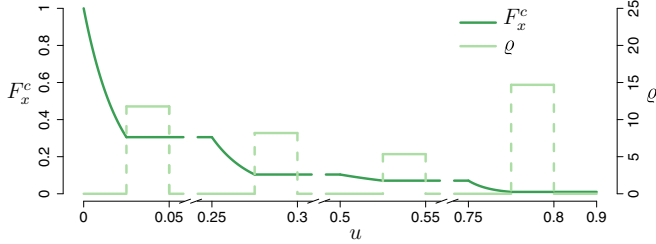
FIG. 1. Graphs of F_x^c for $x \in (0.025, 0.05]$, and of ϱ, in the heterogeneous setting.

off-ramps. To choose a ϱ and family of F_x that correspond to this example, we start by calibrating a finite L model that has a realistic size. Using the calibration in [7] (Sec. 3.1), we take the length of each cell to be about 7 m and our time steps to be 1 s, and we find that $L = 20$ is a suitable choice. The resulting model has geometric features and car velocities that match the realistic ones described in [13] and [14]. We let the on-/off-ramps be located at cells $i = 1, 6, 11, 16$, meaning that only these cells will have nonzero arrival and departure probabilities, while we set the remaining p_i and q_{ij} to zero. We calculate the arrival probabilities p_i at the four on-ramps from the given number of arrivals per hour in the example problem. The departure probabilities q_{ij} are analogously obtained from the given fractions of arriving cars that depart via the off-ramps. The latter requires that we first fix the probability $\prod_{\ell=1}^{L} \bar{q}_{\ell j}$ that a car completes a full circle in the roundabout; we set this probability equal to 1% for every type of car, and then determine the q_{ij} to reproduce the departure behavior of the example.

Now that we have the p_i and q_{ij} for $L = 20$, we can choose our continuum profiles ϱ and F_x accordingly. Recall that we map the full roundabout to the interval $(0,1]$, so that for $L = 20$, each cell corresponds to an interval of length 0.05. We further split each of the four cells $i = 1, 6, 11, 16$ into two halves, where the half that is adjacent to the previous cell corresponds to the off-ramp of the cell, and the other half corresponds to the on-ramp. We now choose ϱ proportional to p_i at the on-ramps and zero elsewhere, and we choose $\theta = \sum_{i=1}^{20} p_i$, so that for $L = 20$, integration of ϱ gives us the correct p_i. As for the departure profiles, we choose the F_x^c to be exponentially decreasing at the off-ramps in analogy with the homogeneous case, and constant in between. Here, the rate of the exponential decrease is chosen such that we obtain the correct q_{ij} for $L = 20$. In Fig. 1 we have plotted the resulting profiles ϱ and a representative from the family $(F_x^c)_{x \in (0.025, 0.05]}$ for illustration. We refer to the profiles ϱ and F_x thus obtained as the *heterogeneous setting* or the *heterogeneous case*. We stress that, although these profiles were calibrated for $L = 20$, we use the same ϱ and F_x in our simulations of the heterogeneous case for other values of L.

In the remainder of the paper, we present various claims about the model. We cannot prove these claims, as we lack an analytic expression for the joint stationary distribution. Instead, we will *support* our claims using simulation in combination with statistical evidence. We use the following structure throughout: first we state the claim and provide the intuition behind it based on the properties of the model, then we

describe an experiment by which we aim to support the claim, provide our support, and finally we draw our conclusions. In each simulation experiment, we initialize (i) the cells according to the marginal stationary probabilities π_{ij}, and (ii) the queues in the empty state. We then let the system run for $4L$ units of time, as we have observed that this is a sufficiently long time interval to safely assume the system has entered the stationary regime.

B. Supporting convergence in distribution statistically

In Sec. VI, we consider the number of empty cells on a segment for a sequence of models in L that we obtain from the continuous arrival and departure profiles, as explained in the preceding section. Among other things, we claim that this quantity converges in distribution to a normal random variable as $L \to \infty$. To empirically verify this claim, we use two methods. The first, which is classical, is to show that the (empirical) distribution functions converge pointwise. The second uses statistical tests and is a method to numerically support convergence in distribution. We explain the second method in this section.

For our explanation, we consider the situation in which $\{\xi_L\}_L$ is a sequence of random variables that converge in distribution to an $N(\mu, \sigma^2)$ random variable. In our method, we use the chi-squared goodness-of-fit test with a confidence level equal to 0.99. We take 10 bins, the boundaries of which are chosen such that every bin contains 10% of the probability mass of the $N(\mu, \sigma^2)$ distribution.

The naive idea for testing convergence to a normal distribution would be to take L large, and apply the χ^2-test with the (L-dependent) hypotheses

$$H_0(L) : \xi_L \overset{d}{=} N(\mu, \sigma^2),$$
$$H_1(L) : \xi_L \overset{d}{\neq} N(\mu, \sigma^2). \tag{3}$$

However, a χ^2-test with these hypotheses does not give useful information on convergence because, in practice, one expects that ξ_L does not have an $N(\mu, \sigma^2)$ distribution for finite L, and therefore one will always reject $H_0(L)$ if the sample size is large enough. The underlying issue is of course that to support convergence in distribution, it is not sufficient to consider a single ξ_L, but one has to consider the full sequence. Our method *exploits* the fact that we can always reject $H_0(L)$ by increasing the sample size. The basic idea is that we compare the sample sizes $M(L)$ for which we first reject $H_0(L)$. If ξ_L converges in distribution, $M(L)$ should diverge to ∞ with L.

To put this idea into practice, we start our procedure by drawing a sample of 50 independent copies of ξ_L. We perform the chi-squared test for goodness-of-fit, with the hypotheses as in (3), which is significant for 50 samples (taking into account the expected counts in each bin). If we reject $H_0(L)$, we set $M(L) = 50$; otherwise, we add another independent copy of ξ_L to our sample, and we perform the chi-squared test again. We keep adding independent copies of ξ_L until we reject $H_0(L)$, at which point we record the size of our sample $M(L)$. Note that $M(L)$ is itself a random variable, so we run this procedure multiple times to estimate the mean $\mathbb{E} M(L)$. Finally, we use linear regression to test whether $\mathbb{E} M(L)$ increases like a power law with L, which implies that

as $L \to \infty$, a diverging number of samples is required to reject $H_0(L)$, thus supporting convergence in distribution.

Our method can, in theory, be applied to every limiting distribution with a set of hypotheses as in (3), using any goodness-of-fit test. For practical applications, however, one has to be able to compute an estimate of $\mathbb{E} M(L)$. For instance, in Sec. VII, we claim convergence in distribution of the total queue length on a segment to a Poisson random variable. There is, however, no statistical test that is powerful enough to distinguish the specific alternative distribution that we are considering. Therefore, one has to use a huge sample size $M(L)$ to reject $H_0(L)$, even for small L, which makes estimating the $\mathbb{E} M(L)$ computationally infeasible in this particular case.

V. MODEL PROPERTIES

In this section, we study the spatial correlations and marginal queue distributions of our model in the finite L regime in equilibrium. Our results also provide information about the behavior in the regime $L \to \infty$, which we study in more detail in Secs. VI and VII.

A. Spatial correlations

Our roundabout model can be seen as a system of particles moving over a one-dimensional circular lattice. Moreover, the update rules are local, so that correlations in the model arise via nearest-neighbor interactions. It is, therefore, conceivable that the correlations decay geometrically in the distance between cells. To investigate this idea, denote by C_i the state of cell i and by Q_i the state of queue i in equilibrium. For states of the cells to contribute symmetrically to the correlations, we let

$$\widetilde{C}_i := [(C_i - i) \mod L] + 1$$

when $C_i \neq 0$, and $\widetilde{C}_i := C_i$ if $C_i = 0$. Thus, $\widetilde{C}_i$ measures the forward distance to the cell where the car that occupies cell i entered the roundabout. Now, our claim is as follows:

Claim 1. The correlation between the random variables $\widetilde{C}_i$ and $\widetilde{C}_{i+k}$ decreases in k for each $i \in \{1, \ldots, L\}$, and is bounded above, uniformly in both i and L, by a function that decreases geometrically with k. The same statement is true for the correlations between $\widetilde{C}_i$ and Q_{i+k}, and for the correlations between Q_i and Q_{i+k}.

To support Claim 1, it is sufficient for the sample correlation to be geometrically decreasing, starting from some distance $k \geqslant 1$. To verify this, we estimate the mean sample correlation coefficient between pairs of cells and/or queues, from a sample of 100 correlation coefficients, each estimated from a simulated data set of size 64×10^4. To analyze the decay of the, potentially negative, mean sample correlation coefficient on a log scale, we take the absolute value of the 100 samples and consider their mean. We then verify that on a log scale, these mean absolute sample correlations are bounded by a decreasing linear function. However, from known results on the asymptotic distribution of the sample correlation (Ref. [15], Example 10.6), we expect that the variance becomes constant as the correlation tends to zero. As a consequence, in our experiment the mean absolute
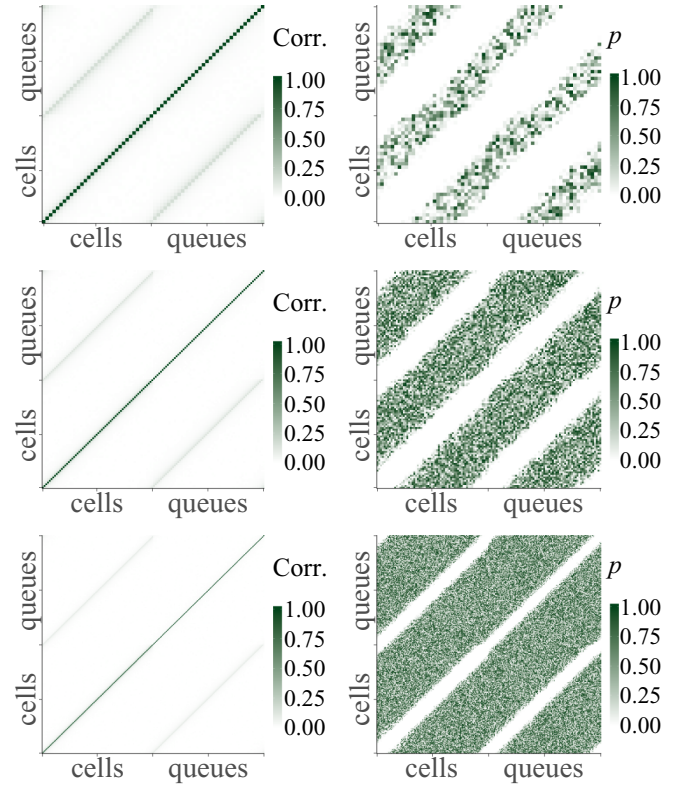

FIG. 2. Heat maps of correlations (Corr.) on the left and corresponding p-values (p) on the right, for the homogeneous case. From top to bottom we have the heat maps for $L = 32$, 64, and 128.

sample correlation will not be a good estimator of the absolute correlation when the correlation is small. To ensure that our estimates are accurate, we therefore only consider points for which the mean sample correlation is at least two standard errors (as determined from the 100 samples) away from zero.

If the correlations do decay geometrically, cells and/or queues that are "sufficiently far apart" are approximately independent. To verify this, we also perform a statistical test of independence. We use the statistic $t = r\sqrt{(n-2)/(1-r^2)}$, where r is the correlation coefficient and n is the sample size. For generally distributed independent random variables and large n, the t statistic can be shown to have a Student's t distribution with $n - 2$ degrees of freedom (Ref. [15], Sec. 26.20). In our experiment, we take $n = 10^6$ and use t to test whether the sample correlations are significant. We aim to show that the correlations are significant over a constant distance independent of L, thus further supporting the claim of geometric decay, uniformly in L.

Support of Claim 1. We consider the homogeneous case first. In Fig. 2 we show heat maps of the correlations and their corresponding p-values between cells and queues for $L = 32$, 64, and 128. Both axes represent a vector containing first the cells, indexed from 1 through L, and then the queues, indexed from 1 through L. First of all, notice that nontrivial correlations do exist, and that for each L they are significant for certain pairs of cells and queues. This confirms that a product-form stationary distribution does not apply, as pointed out earlier. However, we also see that the dependence is not very strong, since (although they are significant according
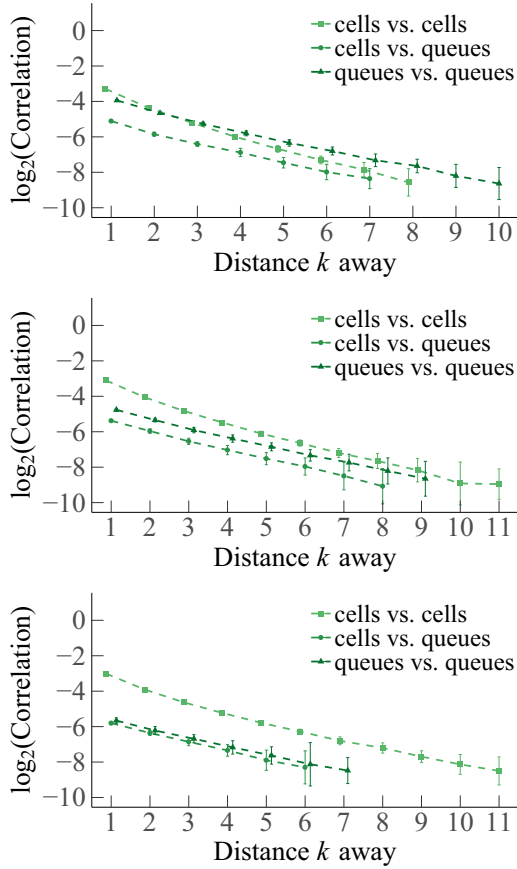
FIG. 3. Decay of correlations, on a log-scale, for the homogeneous case. From top to bottom we have $L = 32$, 64, and 128. For clarity of the figure, the graphs have been shifted horizontally by a small value.

FIG. 4. Heat maps of correlations (Corr.) on the left and corresponding p-values (p) on the right, for the heterogeneous case. From top to bottom we have the heat maps for $L = 32$, 64, and 128.

to the p-values) the correlations between neighboring cells and/or queues are small. Furthermore, we observe that p-values are only significant for correlations between cells and queues that are at most (about) a distance 10 away from each other. This distance is more or less constant in L, which supports our claim that the rate of the decay is uniform in L.

In Fig. 3 we have plotted the mean absolute value of the sample correlations between a cell or queue and neighboring downstream cells or queues, for $L = 32$, 64, and 128 starting from distance $k = 1$, with the corresponding standard error represented by error bars. We have tested for a linear relationship by applying linear regression, yielding $R^2 \approx 0.99$ for every line. We therefore deduce that the decrease is linear, and we can conclude that the mean absolute correlations decay geometrically. Furthermore, we see that the behavior is homogeneous in L. Based on the above, we conclude that our experiments support Claim 1 numerically in the homogeneous case.

For the heterogeneous case, we likewise present a set of heat maps of the correlations and their corresponding p-values in Fig. 4. As some queues are by construction empty in the heterogeneous case, their correlations are depicted in gray in the heat maps. As in the homogeneous case, the results of our simulations numerically support Claim 1. To analyze the decay of the correlations, we have also plotted on a log
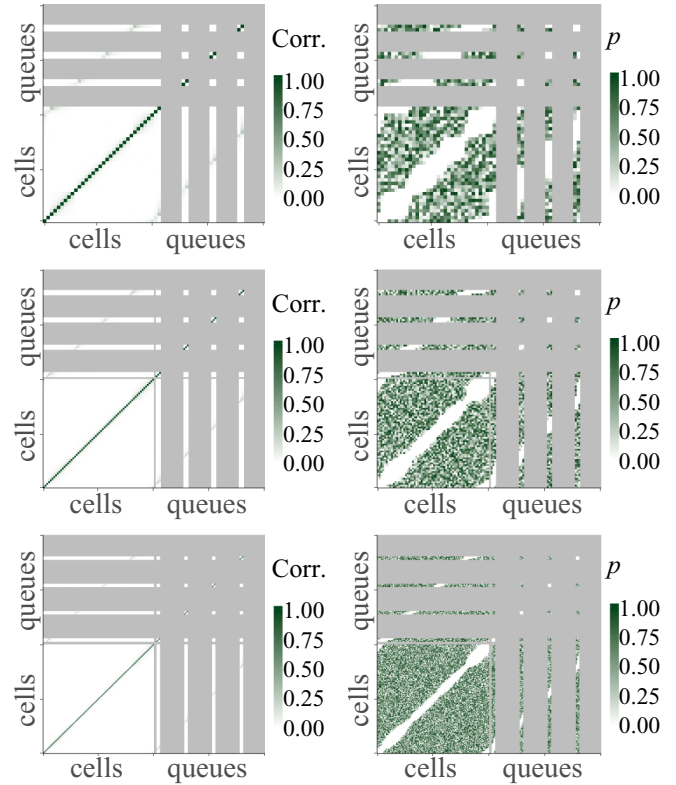
scale, for the first four cells that are a distance $L/8$ apart from each other, their mean absolute correlations with neighboring upstream cells, and their standard errors, as a function of the distance; see Fig. 5. We have applied linear regression, which gave $R^2 \approx 0.99$ for every graph, except for the graph of cell 1 for $L = 64$, which has $R^2 \approx 0.94$. The results confirm a linear decay on a log scale. Therefore, as in the homogeneous case, we find numerical support for Claim 1.

B. Queue distribution

A natural quantity to study is the (marginal) queue length distribution of the system. Because of the dependencies in the system, one cannot derive the marginal queue length distribution analytically; likewise, no mean-value analysis is possible to capture the mean queue length. However, because of the weak dependence, one would expect the queue distribution to approximately have a geometric tail. We therefore claim the following:

Claim 2. All queues have marginal stationary distributions with a tail that is close to geometric.

To verify Claim 2, we have simulated the roundabout for $L = 256$. To estimate the tail of the queue distributions in a sample of size $n = 10^6$ sufficiently accurately, we have to scale the p_i by a factor α in both the homogeneous and the heterogeneous cases. We choose α such that $\pi_{i0}(\alpha) - \alpha p_i \approx 0.1$ for each $1 \leqslant i \leqslant L$. From our data, we estimate the marginal distributions of a set of queues with equal distance between them, and we analyze the tail.
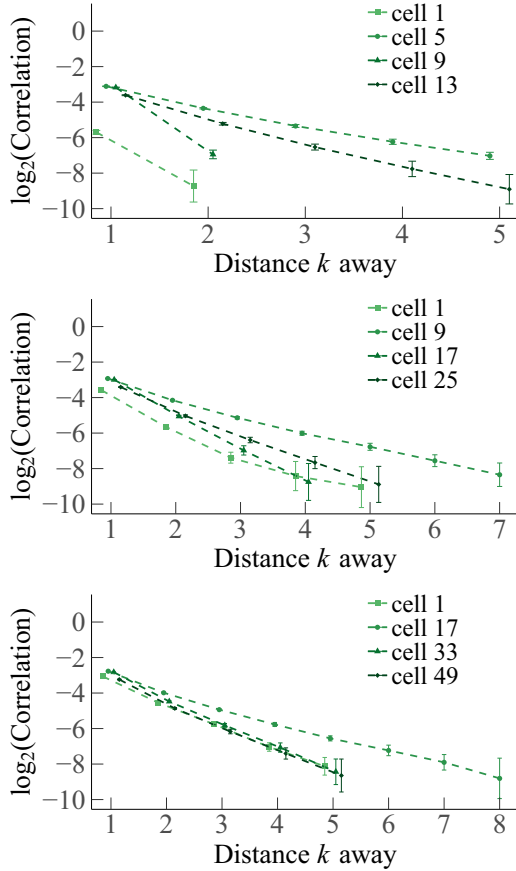
FIG. 5. Decay of correlations, on a log-scale, for the heterogeneous case. From top to bottom we have $L = 32$, 64, and 128. For clarity of the figure, the graphs have been shifted horizontally by a small value.

Support of Claim 2. The results in the homogeneous case are shown in Fig. 6 (left), where λ_{ik} on the vertical axis denotes the stationary probability of the event in which queue i has length k. The figure shows the distribution on a log scale along with its regression line. The slight deviation from the linear relation for small k shows that the distribution is not exactly geometric. However, we observe that the tail is indeed geometric, as the plot is very close to the regression
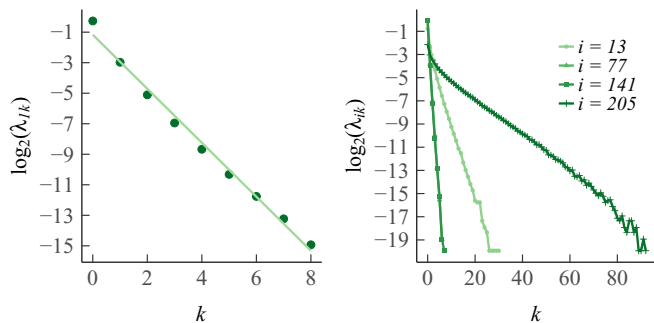

FIG. 6. Marginal queue distribution on log scale for the homogeneous case (left) and heterogeneous case (right), along with the best-fit line for the homogeneous case.

line and linear in the tail, until the estimation errors kick in, thus confirming Claim 2.

For the heterogeneous case, Fig. 6 (right) shows the results on a log scale. That is, we have plotted the distribution of one queue in each of the four arrival zones (i.e., the four on-ramps into the roundabout) for $L = 256$. The legend indicates which queues are considered. We see that each distribution is close to a linear decay on a log scale for k above, say, 4. For $i = 205$, there seems to be a small deviation from a linear line in the tail of the distribution, though performing linear regression yields an R^2 equal to 0.9902. Thus the analysis indicates that, in practice, the distribution can be considered as having geometrically vanishing tails, supporting Claim 2.

VI. SCALING LIMIT FOR CELLS

In this section, we formulate claims about the stationary state of the cells in the regime $L \to \infty$. More specifically, we claim that for each division of the roundabout into segments, the occupation of these segments follows a joint Gaussian distribution in the limit. This Gaussian limit provides an approximation to the stationary distribution of the number of occupied cells on every segment of the roundabout. This knowledge is particularly useful when designing the roundabout; for instance, a performance target could concern the maximum utilization of the roundabout.

We first introduce some notation. Let T_k^L be the random variable that counts the number of vacant cells up to cell k. That is, with C_i the state of cell i, and δ_{jk} the Kronecker delta (i.e., $\delta_{jk} = 1$ if $j = k$, and $\delta_{jk} = 0$ if $j \neq k$),

$$T_k^L := \sum_{i=1}^{k} \delta_{C_i, 0}.$$

Observe that this is a sum of 0-1 random variables with expectations π_{i0}. For $x \in (0, 1]$, write $\pi_L(x) := \pi_{\lceil xL \rceil, 0}$ and $\sigma_L^2(x) := \pi_L(x)[1 - \pi_L(x)]$. Put

$$s_L^2 := \frac{1}{L} \sum_{i=1}^{L} \sigma_L^2(i/L) = \int_0^1 \sigma_L^2(x) dx, \qquad s_L \geqslant 0$$

and

$$t_k^L := \frac{1}{L s_L^2} \sum_{i=1}^{k} \sigma_L^2(i/L) = \frac{1}{s_L^2} \int_0^{k/L} \sigma_L^2(x) dx.$$

Now let $T^L : [0, 1] \to \mathbb{R}$ be the random continuous function that is linear on each interval $[t_{k-1}^L, t_k^L]$, $k = 1, \ldots, L$, and has values

$$T^L(t_k^L) = \frac{T_k^L - \mathbb{E}(T_k^L)}{\sqrt{L s_L^2}}$$

at the points of division. Then our claim is as follows:

Claim 3. As $L \to \infty$, T^L converges in distribution to a time-inhomogeneous Brownian motion $\widehat{T}$ on [0,1] with the representation

$$\widehat{T}(t) = \int_0^t \eta(u) dB_u,$$

interpreted as an Itô integral with respect to a standard Brownian motion B, where η is a deterministic continuous function on $[0,1]$.

We write "time-inhomogeneous," where obviously in this context "time" refers to the position on the roundabout.

Remark 4.1. Instead of counting vacant cells, one could also count cells containing a car of a type between $\lceil aL \rceil$ and $\lceil bL \rceil$, for fixed a and b satisfying $0 < a < b \leqslant 1$. The corresponding random continuous function again converges to a time-inhomogeneous Brownian motion.

The intuition behind the claim is as follows. If the 0-1 variables in the definition of T_k^L were independent, T^L would converge to standard Brownian motion by an extension of Donsker's theorem (Ref. [16], Exercise 8.4). Unfortunately, as stressed before, the cells are not independent. However, we have seen in Sec. V that the correlations between cells are geometrically decaying in the distance between them, and that cells that are "sufficiently far apart" are nearly independent. Hence, one still expects convergence to a (time-inhomogeneous) Brownian motion.

In particular, we expect that nonoverlapping increments of the random function T^L become asymptotically independent (as L grows). Moreover, since the central limit theorem still holds for sequences of random variables that are nearly independent when they are far away from another (e.g., see Ref. [17], Theorem 27.4, for the stationary case), we expect that the increments converge in distribution to zero-mean normal random variables.

As for the covariance matrix between increments, we expect first of all that

$$\mathrm{Var}(T^L(t)) = \frac{1}{Ls_L^2} \sum_{i=1}^{\lfloor tL \rfloor} \mathrm{Var}(\delta_{C_i,0})$$

$$+ \frac{2}{Ls_L^2} \sum_{i=1}^{\lfloor tL \rfloor} \sum_{j=i+1}^{\lfloor tL \rfloor} \mathrm{Cov}\left(\delta_{C_i,0}, \delta_{C_j,0}\right)$$

$$\sim \frac{\lfloor tL \rfloor}{L} + \frac{2\lfloor tL \rfloor a(t)}{L} \rightarrow t + 2ta(t),$$

where $a(t)$ is a constant representing the row average of all correlations in the upper triangular part of the correlation matrix. This sum should be finite because of the geometric decay of correlations. Finally, we expect that the covariances between increments converge to zero, since

$$\mathrm{Cov}(T^L(t) - T^L(s), T^L(s))$$

$$\sim \frac{1}{Ls_L^2} \mathrm{Cov}\left(\sum_{i=\lceil sL \rceil}^{\lfloor tL \rfloor} \delta_{C_i,0}, \sum_{j=0}^{\lfloor sL \rfloor} \delta_{C_j,0}\right)$$

$$\sim \frac{1}{L} \sum_{i=\lceil sL \rceil}^{\lfloor tL \rfloor} \sum_{j=0}^{\lfloor sL \rfloor} \rho_{C_i,C_j} \rightarrow 0.$$

Here, $\sim$ means that both sides have the same limit as $L \rightarrow \infty$, ρ_{C_ℓ,C_k} denotes the correlation coefficient, and the limit is zero since the double sum in the third line is of constant order in L by the geometric decay of correlations.

In view of the above, to support Claim 3, we aim to test (i) that increments of T^L become asymptotically independent
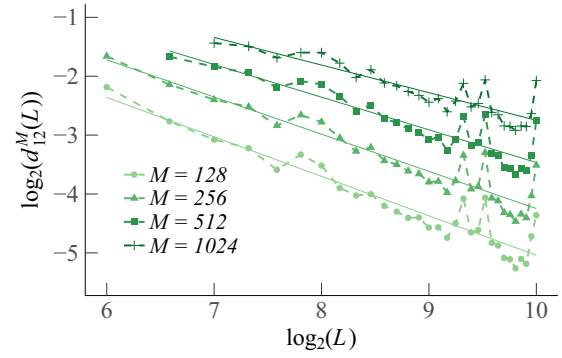

FIG. 7. Graphs of $d_{12}^M(L)$ in the homogeneous case, for $M \in \{128, 256, 512, 1024\}$, along with their best-fit line.

as $L \rightarrow \infty$, and (ii) that they converge in distribution to zero-mean normal random variables.

A. Independence of increments

To verify that the increments of T^L become independent as $L \rightarrow \infty$, we compare the joint distribution of two increments to the product distribution of the marginals. We divide the roundabout of size L into four segments of equal length, and we denote the four increments of T^L on these segments by I_k^L, where $k \in \{1, 2, 3, 4\}$ and the superscript L indicates the dependence on L.

As a measure of the distance between the joint distribution of increments k and j and the distribution one would have if these increments were independent, we define

$$d_{kj}^M(L) = \sup_{|A|=M} \frac{1}{2} \sum_{a \in A} |f_{kj}(a) - f_k(a)f_j(a)|, \qquad (4)$$

Here, the supremum is taken over sets A consisting of M distinct outcomes of the random vector (I_k^L, I_j^L), f_{kj} is the joint density of I_k^L and I_j^L, and f_k and f_j are the respective marginal densities. We note that for $a = (a_k, a_j) \in A$, we interpret $f_k(a)$ as $f_k(a_k)$ and $f_j(a)$ as $f_j(a_j)$. To ensure that the product sample space of I_k^L and I_j^L has at least M elements, L must be large enough [to be precise, $(L/4 + 1)^2 \geqslant M$]. To support Claim 3, we wish to empirically show that $d_{kj}^M(L) \rightarrow 0$ for $k \neq j$ as $L \rightarrow \infty$.

Note that if we replace the supremum in (4) by a supremum over sets A of arbitrary size, then (4) becomes the total variation distance. That distance is not suited for our purposes, because we have to estimate the densities in (4), and the total estimation error grows faster than the total variation distance decreases. This is why we restrict the sum to the M largest contributions in (4).

In our experiment, we take $M \in \{128, 256, 512, 1024\}$ and evaluate $d_{kj}^M(L)$ by estimating the densities $f_{kj}(a)$ and $f_k(a)$ using a simulated sample of size 10^6.

Support of Claim 3. We first consider the homogeneous case. Since neighboring increments have a stronger dependence, as shown above, and because of symmetry, the results of $d_{12}^M(L)$ are representative for all $d_{kj}^M(L)$. Figure 7 shows the estimated $d_{12}^M(L)$ as a function of L on a log-log scale, together with the best-fit line. For every M, we obtain an R^2 between
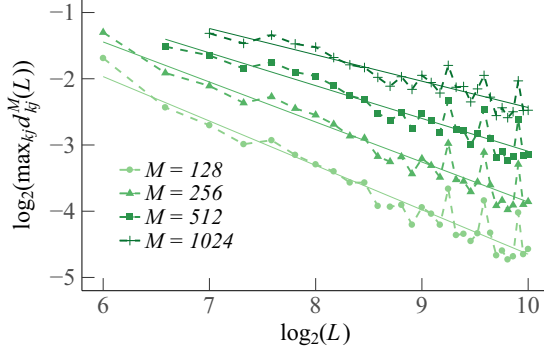
FIG. 8. Graphs of $\max_{kj} d_{kj}^M(L)$ in the heterogeneous case, for $M \in \{128, 256, 512, 1024\}$, along with their best-fit line.

FIG. 9. Graph of $d_1^{\text{sup}}(L)$ for the homogeneous case.

0.78 and 0.92, and a negative slope. Thus we conclude that for each $M \in \{128, 256, 512, 1024\}$, the estimated $d_{12}^M(L)$ decreases in L according to a power law. This is sufficient to also conclude that $d_{12}^M(L) \to 0$ as $L \to \infty$, which supports our claim that the increments of T^L become independent as L becomes large.

For the heterogeneous case, we have plotted the distance $\max_{kj} d_{kj}^M(L)$ (for different M) in Fig. 8. Our conclusions are the same as in the homogeneous case.

B. Distribution of increments

We now focus on supporting the part of Claim 3 stating that the increments of T^L converge in distribution to a normal random variable. For this purpose, we divide $[0,1]$ into N intervals of equal length. For fixed N, we denote the corresponding increments of T^L by I_k^L, and their standard deviations by σ_k^L, where $k \in \{1, \ldots, N\}$. Denote by t_{n-1} the cumulative distribution function of a t-distribution with $n-1$ degrees of freedom.

We use the two methods described in Sec. IV B. However, a complication is that we do not know σ_k^L, and therefore we do not have a complete description of the limiting distribution. Hence, we slightly modify the two methods by considering the random variables $I_k^L/\hat{\sigma}_k^L$, where $\hat{\sigma}_k^L$ is the maximum-likelihood estimator for σ_k^L, estimated from a simulated sample of size $n = 10^6$. Claim 3 implies that, as $L \to \infty$, $I_k^L/\hat{\sigma}_k^L$ converges in distribution to a random variable that has distribution t_{n-1}, and it is this implication that we will support.

With our first experiment, we aim to show that, for every $k \in \{1, \ldots, N\}$,

$$d_k^{\text{sup}}(L) := \left\| \hat{F}_k^L - t_{n-1} \right\|_\infty \to 0$$

as $L \to \infty$, where $\|\cdot\|_\infty$ denotes the supremum norm, and $\hat{F}_k^L$ denotes the empirical distribution function of $I_k^L/\hat{\sigma}_k^L$.

In our second experiment, we use the method that was explained in Sec. IV B. To be precise, we apply the chi-squared goodness-of-fit test, with the hypotheses

$$H_0(L) : I_k^L/\hat{\sigma}_k^L \stackrel{d}{=} t_{n-1},$$

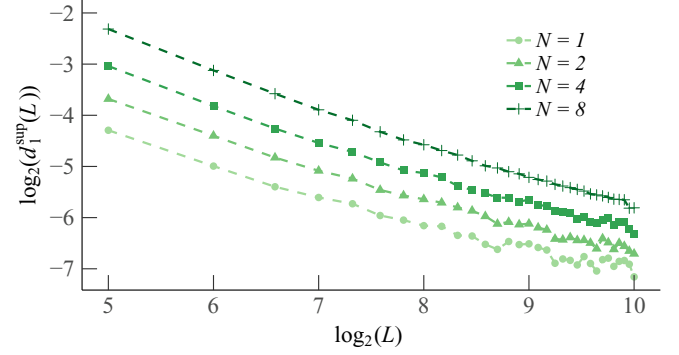$$H_1(L) : I_k^L/\hat{\sigma}_k^L \stackrel{d}{\neq} t_{n-1},$$

to determine $M(L)$. We estimate $\mathbb{E} M(L)$ by repeating the procedure 10^4 times, and we aim to show that $\mathbb{E} M(L)$ diverges as $L \to \infty$.

Support of Claim 3. Consider the first experiment, and the homogeneous case. For $N \in \{1, 2, 4, 8\}$, we have plotted $d_1^{\text{sup}}(L)$ in Fig. 9. By symmetry, the results for $k \neq 1$ are similar. As the graphs are all linear in L on a log-log scale, the distance decreases in L like a power law. This is in turn sufficient to conclude that for each $1 \leqslant k \leqslant N$, $d_k^{\text{sup}}(L) \to 0$ as $L \to \infty$, and thus supports Claim 3.

For the heterogeneous case, Fig. 10 depicts the distance $\max_k d_k^{\text{sup}}(L)$ as a function of L. The results are in line with those of the homogeneous case. Hence, the experiment supports convergence in distribution of the increments of T^L.

Support of Claim 3. Now consider the second experiment. For $N \in \{1, 2, 4, 8\}$ and $k \in \{1, \ldots, N\}$ we have estimated $\mathbb{E} M(L)$ for $L \in \{32, 64, \ldots, 1024\}$. Then, we applied a log-transformation to L and $\mathbb{E} M(L)$, after which we applied linear regression to find the best linear fit. The idea is that if the linear fit on a log-log scale is good and strictly increasing, then $\mathbb{E} M(L)$ is strictly increasing in L via a power law, i.e., $\mathbb{E} M(L) \sim L^\beta$, where β is the slope of the linear fit found by the regression.

The results of the linear regression are given in Table I for the homogeneous case, and in Table II for the heterogeneous case. Here, N and k are as before, "Rsq" and "Rsq_adj" are, respectively, the ordinary and adjusted R^2 from ordinary least squares, F is the F-statistic, and p is its corresponding
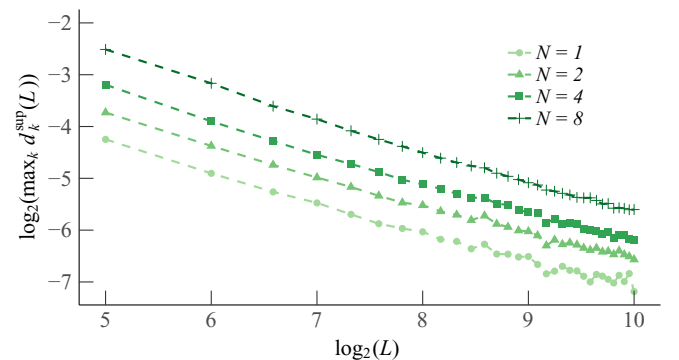

FIG. 10. Graph of $\max_k d_k^{\text{sup}}(L)$ for the heterogeneous case.

TABLE I. Results of the linear regression of L vs estimated $\mathbb{E}\,M(L)$ (homogeneous case).

N	k	Rsq	Rsq_adj	F	p	Intercept	Slope
1	1	0.8134	0.8072	130.7484	1.8457×10^{-12}	1.0406	1.0076
2	1	0.7128	0.7033	74.4703	1.2586×10^{-9}	0.7283	1.0261
2	2	0.7197	0.7104	77.0325	8.7121×10^{-10}	0.7331	1.0274
4	1	0.5816	0.5677	41.7071	3.9042×10^{-7}	1.4803	0.7842
4	2	0.5690	0.5546	39.6035	6.1631×10^{-7}	1.3822	0.8033
4	3	0.5728	0.5586	40.2324	5.3689×10^{-7}	1.4932	0.7814
4	4	0.5797	0.5657	41.3778	4.1895×10^{-7}	1.4924	0.7811
8	1	0.5509	0.5359	36.8022	1.1580×10^{-6}	0.1515	0.9281
8	2	0.5479	0.5328	36.3542	1.2841×10^{-6}	0.1686	0.9252
8	3	0.5435	0.5282	35.7116	1.4914×10^{-6}	0.1776	0.9237
8	4	0.5498	0.5348	36.6344	1.2036×10^{-6}	0.1872	0.9214
8	5	0.5462	0.5311	36.1087	1.3594×10^{-6}	0.1447	0.9289
8	6	0.5428	0.5275	35.6145	1.5257×10^{-6}	0.1627	0.9269
8	7	0.5497	0.5346	36.6159	1.2088×10^{-6}	0.1582	0.9277
8	8	0.5321	0.5165	34.1113	2.1793×10^{-6}	0.3014	0.8971

p-value. The last two columns contain the intercept and slope of the regression line given by ordinary least squares.

The tables show that under the assumption of standard normally distributed residuals, the fit for each pair of N and k is good, since R^2 is large and the p-value from the corresponding F-statistic is very small. Also, the slope is always significantly positive. As explained above, we thus conclude that $\mathbb{E}\,M(L)$ diverges like a power law in L.

In both the homogeneous and heterogeneous cases, we have to verify that the residuals of the regressions are normally distributed, and that the conclusions we draw are therefore valid. To do so, we made QQ-plots for every pair of N and k; the case $N = 4$ and $k = 1$ is given in Fig. 11 for illustration. The data from which these residuals stem are drawn on a log-log scale in Fig. 11 together with the best-fit line. None of the QQ-plots gives us a reason to question the assumption of normally distributed residuals, and hence our conclusions are valid.

TABLE II. Results of the linear regression of L vs estimated $\mathbb{E}\,M(L)$ (heterogeneous case).

| N	k	Rsq	Rsq_adj	F	p	Intercept	Slope
1	1	0.7541	0.7459	92.0002	1.1971×10^{-10}	0.7161	1.0702
2	1	0.6878	0.6773	66.0790	4.4923×10^{-9}	0.5324	0.9724
2	2	0.5639	0.5493	38.7879	7.3848×10^{-7}	2.0480	0.7580
4	1	0.7518	0.7436	90.8835	1.3761×10^{-10}	0.9568	0.8230
4	2	0.6827	0.6721	64.5423	5.7407×10^{-9}	0.3722	0.8814
4	3	0.6955	0.6854	68.5310	3.0624×10^{-9}	0.3669	0.8900
4	4	0.7479	0.7395	88.9982	1.7462×10^{-10}	0.9977	0.8228
8	1	0.6871	0.6767	65.8841	4.6332×10^{-9}	1.0612	0.6820
8	2	0.6306	0.6183	51.2062	5.8243×10^{-8}	0.8349	0.7562
8	3	0.4906	0.4737	28.8981	8.0635×10^{-6}	1.3538	0.6137
8	4	0.4476	0.4292	24.3093	2.8351×10^{-5}	1.6853	0.5714
8	5	0.4880	0.4709	28.5930	8.7378×10^{-6}	1.5911	0.5810
8	6	0.4839	0.4667	28.1235	9.8957×10^{-6}	1.4242	0.6184
8	7	0.6181	0.6053	48.5450	9.6884×10^{-8}	0.7438	0.7548
8	8	0.6540	0.6425	56.7122	2.1412×10^{-8}	0.6693	0.7848
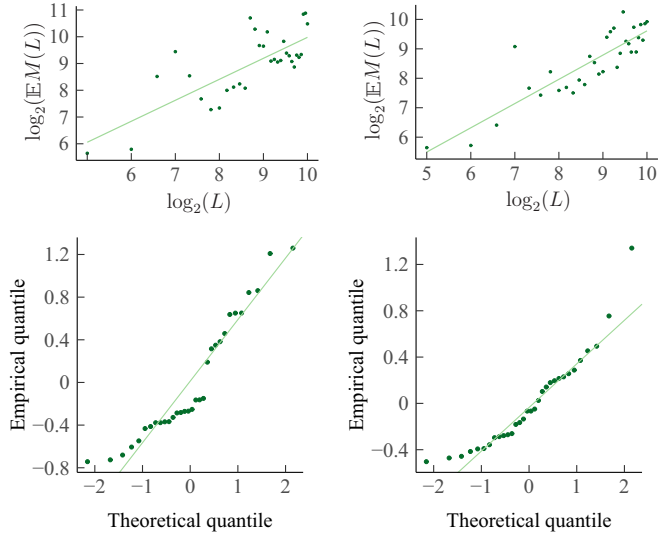
FIG. 11. Illustration results of linear regression. The upper figures show the regression and the lower figures show the corresponding QQ-plots, with the homogeneous case (left) and the heterogeneous case (right).

VII. SCALING LIMIT FOR QUEUES

We now focus on the behavior of the total queue length in a segment of the roundabout, as $L \to \infty$. We claim that, for every subdivision of the roundabout into segments, the sum of the queue lengths within these segments is Poisson-distributed. Similar to our results for the cells, one could use these results for the queues in the design of the roundabout. For example, using the Poisson limit in combination with Little's law, we can approximate mean waiting times; one could thus design the roundabout such that these delays remain within an acceptable bound.

Before we formulate our claim, we introduce some notation. Recall that Q_i denotes the length of queue i in equilibrium. Define $P_0^L = 0$ and

$$P_k^L := Q_1 + \cdots + Q_k, \quad k \geqslant 1.$$

Furthermore, define $P^L : [0, 1] \to \mathbb{N}_0$ by $P^L(u) = P_{\lceil uL \rceil}^L$. We now claim the following:

Claim 4. As $L \to \infty$, P^L converges in distribution to a time-inhomogeneous Poisson process P.

The intuition for this claim stems primarily from studying the behavior of specific quantities in the roundabout model, as $L \to \infty$. We have $p_i = O(1/L)$ and $q_{ij} = O(1/L)$, so that $\pi_{i0} = O(1)$. We write σ_{ikl} for the stationary probability of the event $\{C_i = k, Q_i = l\}$, and recall that λ_{ik} denotes the stationary probability that $Q_i = k$. By considering what happens when we start the Markov chain from the stationary distribution, and let it take one step, one can derive the identities

$$\pi_{i+1,0} = \sum_{j=1}^{L} \pi_{ij} q_{ij} + \sigma_{i00}(1 - p_i), \quad (5)$$

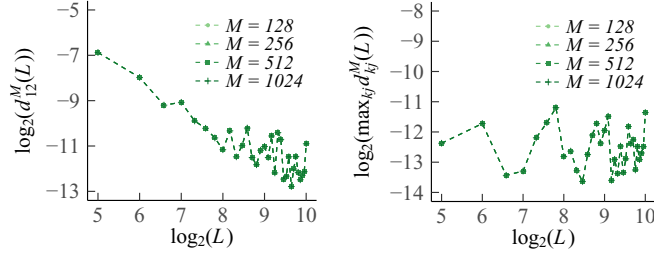$$\lambda_{i0} = \lambda_{i0}(1 - p_i) + \sigma_{i01}(1 - p_i) + \sigma_{i00} p_i. \quad (6)$$

FIG. 12. Graphs of $d_{12}^M(L)$ for the homogeneous case (left) and $\max_{k,j} d_{kj}^M(L)$ for the heterogeneous case (right), for $M \in \{128, 256, 512, 1024\}$.

Furthermore, a calculation shows that (1) and (2) imply

$$\sum_{j=1}^{L} \pi_{ij}(1 - q_{ij}) = 1 - \pi_{i+1,0} - p_i. \tag{7}$$

Combining (7) with (5) and (2) yields

$$\sigma_{i00} = \frac{\pi_{i0} - p_i}{1 - p_i},$$

implying that $\sigma_{i00} = O(1)$. Using that $\sigma_{i01} \geqslant 0$, it then follows from (6) that $\lambda_{i0} = O(1)$ as well.

This line of reasoning fails to determine the order of λ_{ik}, but it is conceivable that $\lambda_{ik} = O(1/L^k)$. The argument behind this is as follows. Since $\pi_{i0} = O(1)$, the time we have to wait for an empty cell is of constant order. For a queue of length k to build up from an empty queue, we need to have at least k arrivals within this constant time. The probability that this happens is of order $1/L^k$, because $p_i = O(1/L)$.

Under the proviso that $\lambda_{ik} = O(1/L^k)$, it follows that the functions P^L behave asymptotically as counting processes. For convergence to a Poisson process, it then suffices that the finite-dimensional distributions converge to those of a Poisson process (see, e.g., Ref. [16], Theorem 12.6). To support Claim 4, we therefore verify below (i) that the increments of P^L become independent as $L \to \infty$, and (ii) that they converge in distribution to a Poisson random variable.

A. Independence of increments

To verify that the increments of P^L become independent, we use the same experiment as the one used for the Gaussian scaling limit. For completeness, we recall its main ingredients, and we introduce some notation. We divide the roundabout into four segments, and we denote the increments of P^L on these segments by J_k^L, where $k \in \{1, 2, 3, 4\}$. We use the metric defined in (4), where f_{kj} is now the joint density of J_k^L and J_j^L, and where f_k and f_j are their respective marginal densities. For $M \in \{128, 256, 512, 1024\}$, we aim to show that for $k \neq j$, $d_{kj}^M(L) \to 0$ when $L \to \infty$.

Support of Claim 4. In the left plot of Fig. 12 we show the graph of the estimates of $d_{12}^M(L)$ as a function of L. By symmetry, and because neighboring increments have the strongest dependence, it is enough to consider $k = 1$ and $j = 2$ in the homogeneous case. First, from the figure we establish that our estimate is the same for each M, which is due to the small support of the empirical distributions. From the linearity of the plot we see that $d_{12}^M(L)$ is decreasing according

to a power law, which is sufficient for $d_{12}^M(L) \to 0$ as $L \to \infty$. Finally, we also see that $d_{12}^M(L)$ is already small for $L = 32$ and quite quickly becomes too small to estimate accurately with our sample size, meaning that the effect of the variance kicks in quite quickly. Rather than negating our findings, this actually makes our conclusion stronger, since the queues are already only weakly dependent for small L.

For the heterogeneous case, we plotted $\max_{k,j} d_{kj}^M(L)$ as a function of L in the right panel of Fig. 12. Again, the function does not depend on M. The dependencies are systematically small, so that we cannot show that $\max_{k,j} d_{kj}^M(L) \to 0$ as $L \to \infty$. However, the results still support independence of the increments of P^L in the limit, since the dependence is already negligible for $L = 32$.

B. Distribution of increments

To verify that the increments of P^L are Poisson-distributed, we use an experiment analogous to the one used in supporting Claim 3. Because we do not have a statistical test with enough power to apply the second method from Sec. IV B, we can only use the first method here, which looks at the distance between the empirical distribution function and a Poisson distribution. We divide the roundabout into N segments of equal length, where $N \in \{1, 2, 4, 8\}$. Each of these segments corresponds to an increment of P^L that, for fixed N, we denote by J_k^L with $k \in \{1, \ldots, N\}$. Our claim is that in the limit $L \to \infty$, J_k^L has a Poisson distribution with some parameter ν.

For the homogeneous case, we estimate ν by the maximum-likelihood estimator $\hat{\nu} = \bar{P}^{1024}(1)$, the bar denoting the sample mean. We set $\hat{\nu}_k = \hat{\nu}/N$ for each k. In the heterogeneous case, we estimate the parameter separately for each increment, as we do not expect a homogeneous Poisson process; so in this case, we have $\hat{\nu}_k = \bar{J}_k^{1024}$.

The experiment is designed to support that

$$d_k^{\text{sup}}(L) := \left\| \hat{G}_k^L - \text{Ps}(\hat{\nu}_k) \right\|_\infty \to 0$$

for $1 \leqslant k \leqslant N$ as $L \to \infty$. Here, $\hat{G}_k^L$ denotes the empirical distribution function of J_k^L, and $\text{Ps}(\hat{\nu}_k)$ denotes a Poisson distribution with parameter $\hat{\nu}_k$. To justify that we use $\hat{\nu}_k$ as the parameter, we estimate $\mathbb{E} \sum_{i=1}^{k} J_i^L$ for each $L \in \{32, 64, \ldots, 1024\}$ via the sample mean, and numerically verify that the sample mean converges in L.
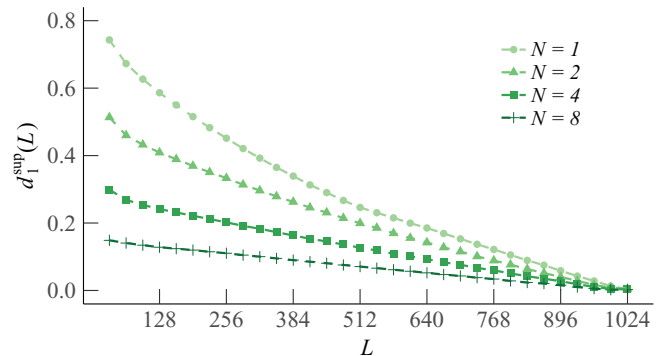

FIG. 13. Graph of $d_1^{\text{sup}}(L)$ for $N \in \{1, 2, 4, 8\}$ (homogeneous case).
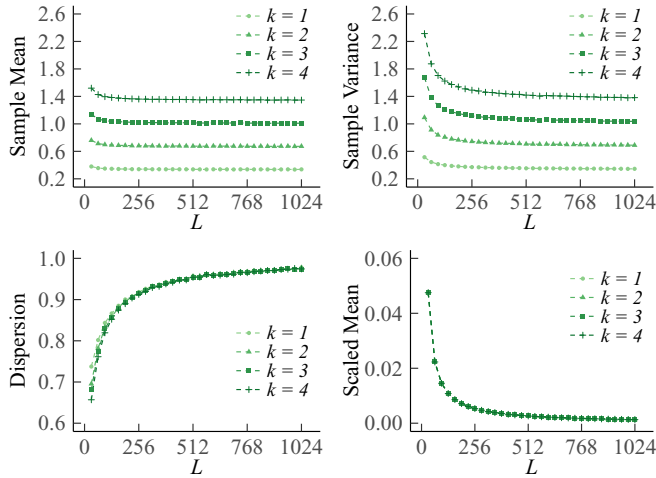
FIG. 14. Poisson characteristics for the increments $\sum_{i=1}^{k} J_i^L$, for $k \in \{1, 2, 3, 4\}$ and $N = 4$, in the homogeneous case. Shown are the means (upper left), the variances (upper right), the dispersions (lower left), and the scaled means (lower right).

FIG. 16. Poisson characteristics for the increments $\sum_{i=1}^{k} J_i^L$, for $k \in \{1, 2, 3, 4\}$ and $N = 4$, in the heterogeneous case. Shown are the means (upper left), the variances (upper right), the dispersions (lower left), and the scaled means (lower right).

Support of Claim 4. We present the homogeneous case first. In Fig. 13 we show the graph of $d_1^{\text{sup}}(L)$ for $N \in \{1, 2, 4, 8\}$, which supports our claim that $d_1^{\text{sup}}(L)$ tends to zero. For $k \neq 1$ the results are equivalent due to symmetry. In Fig. 14 we show the behavior of the sample means, sample variances, and sample dispersions of $\sum_{i=1}^{k} J_i^L$, and the scaled sample means $\sum_{i=1}^{k} \bar{J}_i^L / (\frac{Lk}{N})$, for $k \in \{1, 2, 3, 4\}$ and $N = 4$. Observe from the first set of graphs that the sample means converge, so that we can indeed use $\hat{\nu}$ as an estimate of the true Poisson parameter. Furthermore, the variances also converge. The corresponding dispersions tend to 1, which is indicative of the underlying random variable being Poissonian, thus providing additional support for our claim. Finally, the graph of the scaled means shows that the infinitesimal contribution of each queue goes to zero, but is equal for every subdivision of N increments. Hence, even for L relatively small, P^L behaves like a Poisson process.

For the heterogeneous case, for $N \in \{1, 2, 4, 8\}$, we have plotted $\max_k d_k^{\text{sup}}(L)$ as a function of L in Fig. 15. Figure 16 shows the sample means, variances, dispersions, and scaled
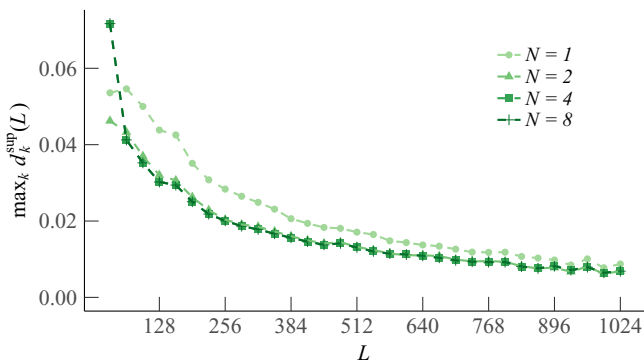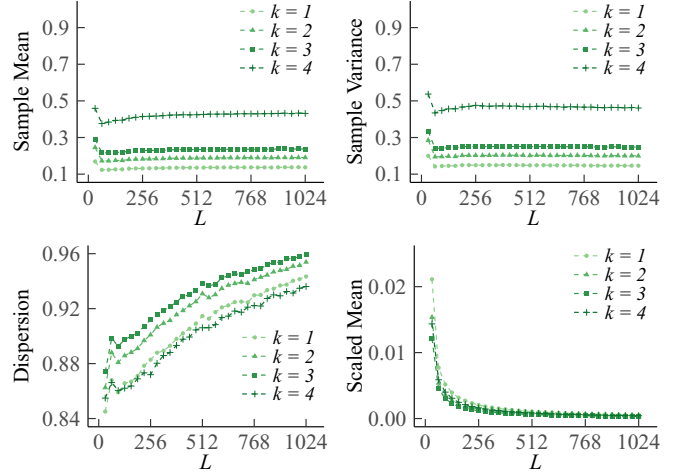
means for $N = 4$. We see that the conclusions from the homogeneous case carry over to the heterogeneous counterpart.

VIII. CONCLUSION

Existing analytical papers on roundabout modeling tend to leave out relevant model features (on-/off-ramps, entry behavior, etc.) to facilitate the derivation of closed-form expressions. The obvious alternative is to realistically model the underlying dynamics, but to resort to simulation. The primary objective of our paper was to develop a roundabout model that included relevant (geometric) properties while still allowing mathematical analysis.

We have proposed a roundabout model that models the cars' circulating behavior and has queueing at the on-ramps. The model is highly flexible; its parameters can be directly calibrated to measurements. We find an explicit expression for the marginal stationary distribution of the cells of which the roundabout consists. As it turns out, the cells and the queues are dependent, so that obtaining a joint stationary distribution remains out of reach. The experiments, however, show that dependencies are typically small, thus leading to various approximations. These approximations are tested in depth, and supported by numerical evidence. They can be used when designing the roundabout in such a way that delay or occupation measures are kept below a maximum allowable level.

Our model includes many features that were not incorporated in previously studied models. Nonetheless, various extensions can be thought of. One could, for instance, make the entry behavior and congestion on the circulating ring more realistic (so as to capture the effect that cars stop moving when cells in front of them are occupied). Importantly, we do believe that, while their functional forms might change, our findings generalize to more realistic models; the underlying arguments and/or techniques are not affected when one includes these features. In addition, a challenging research direction could relate to modeling roundabouts in networks.

FIG. 15. Graph of $\max_k d_k^{\text{sup}}(L)$ for $N \in \{1, 2, 4, 8\}$ (heterogeneous case).

[1] S. Maerivoet and B. De Moor, arXiv:physics/0507126.

[2] F. van Wageningen-Kessels, H. Van Lint, K. Vuik, and S. Hoogendoorn, EURO J. Transp. Logist. **4**, 445 (2015).

[3] S. Maerivoet and B. De Moor, Phys. Rep. **419**, 1 (2005).

[4] M. E. Fouladvand, Z. Sadjadi, and M. R. Shaebani, Phys. Rev. E **70**, 046132 (2004).

[5] R. Wang and H. J. Ruskin, Comput. Phys. Commun. **147**, 570 (2002).

[6] R. Wang and M. Liu, in *International Conference on Computational Science* (Springer, Berlin, Heidelberg, 2005), pp. 420–427.

[7] N. P. Belz, L. Aultman-Hall, and J. Montague, Transp. Res. Part C **69**, 134 (2016).

[8] A. Flannery, J. P. Kharoufeh, N. Gautam, and L. Elefteriadou, Estimating delay at roundabouts, *TRB Annual Conference Proceedings* (Transportation Research Board, Washington, DC, 2000).

[9] A. Flannery, J. P. Kharoufeh, N. Gautam, and L. Elefteriadou, Civil Eng. Environ. Syst. **22**, 133 (2005).

[10] J. Tanner, Biometrika **49**, 163 (1962).

[11] D. Heidemann and H. Wegmann, Transp. Res. Part B **31**, 239 (1997).

[12] M. E. Foulaadvand and P. Maass, Phys. Rev. E **94**, 012304 (2016).

[13] HCM2010, *Highway Capacity Manual Volumes 1-4* (U.S. National Research Council, Transportation Research Board, Washington, DC, 2010).

[14] R. Akçelik, An assessment of the Highway Capacity Manual 2010 roundabout capacity model, *TRB International Roundabout Conference* (Transportation Research Board, Carmel, Indiana, USA, 2011).

[15] M. Kendall and A. Stuart, *The Advanced Theory of Statistics* (Hafner, New York, 1961), Vols. I and II.

[16] P. Billingsley, *Convergence of Probability Measures* (Wiley, New York, 2013).

[17] P. Billingsley, *Probability and Measure* (Wiley, New York, 2008).